Transportation Geotechnics 36 (2022) 100825

Contents lists available at ScienceDirect

Transportation Geotechnics

journal homepage: www.elsevier.com/locate/trgeo

Self-inspection system for ground anchors monitoring on long-term load change

Shih-Hao Cheng [a,*], Shi-Shuenn Chen [b], Kuo-Hsin Yang [c]

[a] Taiwan Building Technology Center, National Taiwan University of Science and Technology, Address: 43, Sec. 4, Keelung Rd., Taipei City, Taiwan, ROC

[b] Department of Civil and Construction Engineering, National Taiwan University of Science and Technology, Address: 43, Sec. 4, Keelung Rd., Taipei City, Taiwan, ROC

[c] Department of Civil Engineering, National Taiwan University, Address: 1, Sec. 4, Roosevelt Rd., Taipei City, Taiwan, ROC

ARTICLE INFO

Keywords:
Self-inspection
Ground (smart) anchor
Corrosion-protected assembly
Load monitoring
Restressing component

ABSTRACT

This study proposes a newly method for inspecting the load changes of ground anchors (or call smart anchor assembly). The smart anchor operates in a similar fashion to that of the tell-tale load cell in principle. It only requires the components used in a typical anchor assembly and consists of only one extra strand as the reference strand, which is not engaged on the anchorage. For this method, when the anchor load changes, the anchorage moves and a relative displacement between the reference strand and anchorage is generated. Based on the measured relative displacement and the characteristics of ground anchor, the change in anchor load can be approximately calculated. At the same time, by the use of linear potentiometer, data logger, power supply, and data transmitter, automating the self-inspection function of load monitoring can also be achieved. The reliability of automatic load monitoring capabilities of the smart anchor was confirmed by sensing tests performed on field anchors. It would reduce maintenance costs and the engineers can contribute their expertise to value tasks. Lastly, when there's need to increase anchor loading, reference strands can also serve as restressing component. This can extend the service life of ground anchors and achieve the goal of sustainable development.

Introduction

Over the past 10 years, a comprehensive ground anchor inspection program has been practiced in Taiwan. According to the works reported that the inspection results of hundreds of thousands of existing ground anchors on slopes in Taiwan and discovered that most ground anchors can effectively stabilize slopes under normal conditions. However, because of the effect of groundwater, improper design, and construction defects, a small number of ground anchors exhibited corrosion in their steel strands, which results in damage to anchored slopes [1–4]. The result mentioned above highlights the importance of evaluating and tracking the behaviours of anchored slopes. Landslides on natural slopes is mainly induced by heavy rainfall or earthquakes, and it occurs instantly and quickly; therefore, the provision of effective early warning is difficult. By contrast, the sliding of anchored slopes or other artificially reinforced slopes is mostly progressive and is likely to occur without rainy or external force. Through effective monitoring equipment and reliable early warning systems, abnormal situations can generally be detected, and necessary remediation can be implemented before damage occurs [5].

Typically, stressing load is applied to the ground anchors on anchored slopes to stabilize potential sliding soil blocks. Therefore, in the life cycle of an anchored slope, the level of load can be maintain and the trend of load change (increasing or decreasing) on ground anchors directly represent the performance of the ground anchors and indirectly represent the stability or safety of the slope. Although the lift-off procedure and some sensing devices (e.g., electrical load cells, strain gauges, fiber optic sensors, and elasto-magnetic technology) exist to examine load level and load change [6,7], most of these measures must be performed using special stressing equipment or additional sensors. Furthermore, additional limitations in equipment operation expertise, equipment durability and weather resistance, and difficulty in sensor installation may restrict the measurements that can be performed. When the recorded data feature substantial variability and inconsistency, assessments of the state of anchored slopes become difficult and less reliable.

In order to improve the corrosion protection of ground anchors and solve the restrict problems of load tracking, this study proposed a new anchor assembly method (called smart anchor production), and elaborates the smart anchor features of self-inspection on loading changes and

* Corresponding author.
E-mail addresses: shcheng@mail.ntust.edu.tw (S.-H. Cheng), sschen@mail.ntust.edu.tw (S.-S. Chen), khyang@ntu.edu.tw (K.-H. Yang).

https://doi.org/10.1016/j.trgeo.2022.100825
Received 11 April 2022; Received in revised form 26 July 2022; Accepted 27 July 2022
Available online 30 July 2022

restressing capabilities. The following content indicates that the smart anchor is a fully corrosion-protected ground anchor. The assembly process reduces possible sources of groundwater leakage associated with the use of conventional anchors without having to use new construction materials, change conventional construction practices, or employ new construction equipment [8,9]. Furthermore, we incorporated the concept of tell-tale devices [10]. That is, an additional strand was omitted to lock-in wedges (i.e., the reference strand, which is not stressed) alongside the stressed strands with lock-in wedges. In this manner, we could estimate anchor load change based on the relative displacement between the exposed length of the stressed strands and the reference strand, along with the known effective free length, material characteristics, and cross-section properties of the ground anchor [11,12]. In essence, the smart anchor aims to achieve self-inspection of loading change through the mechanical properties of anchor components. An advanced automatic loading inspection system can be created by including automation devices (e.g., a linear potentiometer), a data logger, a power supply, and a data transmitter to the reference strand. To demonstrate the applicability and practicality of the automatic loading inspection capabilities of the smart anchor, this study performed a field test and the objectives that include (1) to introduce the smart anchor assembly and self-inspection functionality of loading change, (2) to describe the composition of automatic loading inspection capabilities of the smart anchor, and (3) to demonstrate the reliability of automatic self-inspection system for long-term load monitoring.

Smart anchor assembly and self-inspection functionality

Ground anchors stabilize slopes and prevent them from sliding by converting the stressing strands into compression force on the ground. The key elements of a ground anchor are (1) the ground anchor body, composed of a free-length and a fixed-length section; (2) the anchor head; and (3) relevant accessories. The design principle of all ground anchors are the same in essence; however, the assembly materials and construction methods are flexible [13]. The following will explanation the assembly details of smart anchor:

Address the water leakage sources of conventional ground anchor

Since the incident of anchored slope failed along Taiwan Freeway 3 in 2010, the functioning of the approximately 100,000 ground anchors in Taiwan has been inspected. The inspection results revealed that ground anchor corrosion is a common problem, and the cause of the corrosion is the contact of steel strands with rainwater or groundwater [1,4,12]. As displayed in Fig. 1, possible sources of water leakage into strands of conventional ground anchors are (1) the open tip of the strand assembly (Fig. 1a), (2) the joint (sealing device) between the smooth sheath of the free-length section and corrugated sheath of the fixed-length section (Fig. 1b), and (3) the ungrouted void under the anchorage head (Fig. 1c). To delay the development of corrosion in existing anchors and maintain their residual load, a set of standard inspection procedures and remedial measures has been established in Taiwan [8,12]. However, new anchors must be reinforced through fundamental corrosion protection, which can be conducted through the following measures (1) replace steel strands with corrosion-resistant materials, such as glass fiber–reinforced polymer strands, carbon fiber–reinforced polymer strands, or epoxy-coated and epoxy-filled strands; and (2) use factory assembly anchors rather than on-site assembly anchors because factory assembly anchors have more integrity and the details of component corrosion can be controlled more precisely. Nevertheless, these two measures have limitations, including an increase in cost due to the new materials used, the need to adjust assembly techniques, the inability to adapt to individual geological, and a change in construction techniques, which have not been commonly applied in Taiwan's ground anchor industry. In this study, we rectified the water leakage problem that occurs in conventional anchors by adjusting the assembly procedures without having to incorporate any new materials or construction techniques.

The smart anchor assembly method emphasizes fully corrosion-protected (Fig. 2a). The first adjustment introduced by the method was to apply a closed-tip strand assembly and change the sequence of cement grouting. It grouted the anchor hole first and inserted the strand assembly afterward to block possible sources of groundwater intrusion (Fig. 2b). Second, we removed the seal device between the fixed-length and free-length sections, where water leakage may occur, and encased the entire length of the steel strands with a corrugated sheath. Cement was grouted from the bottom of the corrugated sheath to the anchor head, facilitating the cement grouting in the corrugated sheath. However, to keep the stress transmission and extension of the free-length section, each strand separately in the free-length section was coated with grease and covered with a small polyethylene (PE) sheath. Heat-shrink tubes sealed the bottom of the small PE sheaths to isolate the

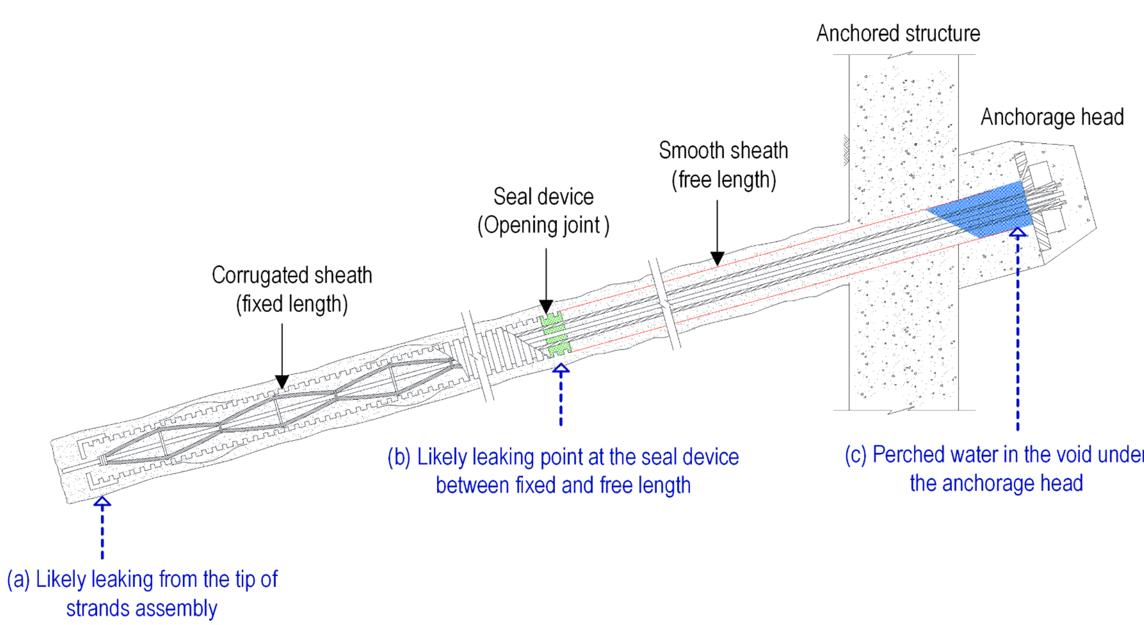

Fig. 1. Possible sources of water leakage into strands of conventional ground anchors in Taiwan.

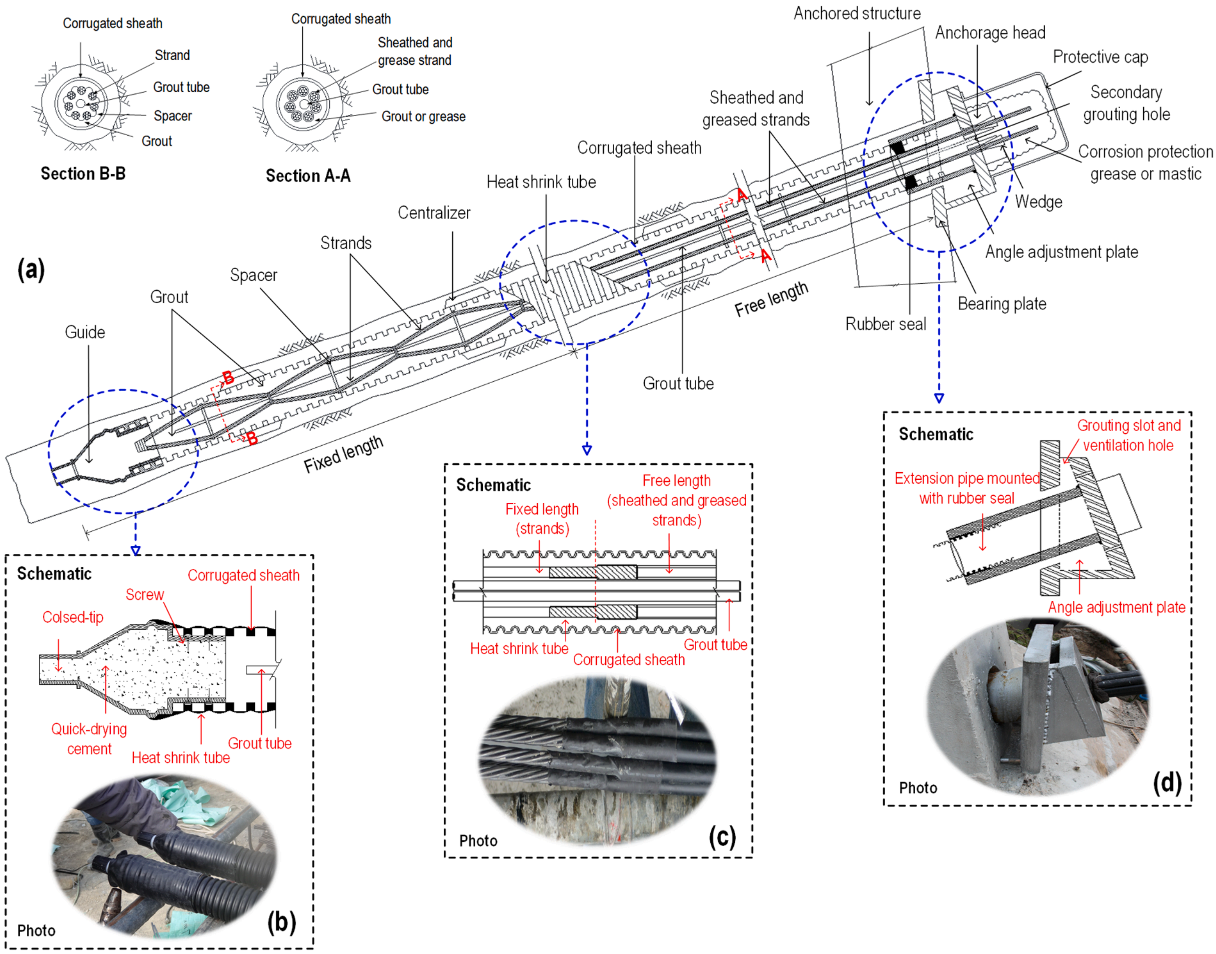

Fig. 2. Production of the smart anchor: (a) schematic of the fully corrosion-protected production; (b) details and photo of the closed-tip strand assembly; (c) details and photo of the opening joint removed; (d) details and photo of the custom bearing plate assembly under the anchorage head.

cement inflow from fixed-length, which avoid affected the extension of the free-length strand (Fig. 2c). A third possible source of water intrusion is the ungrouted void beneath the anchorage head. It employed a custom bearing plate assembly to prevent this. The bearing plate assembly consists of an extension pipe mounted with a rubber seal to prevent groundwater from flowing into the sheath, and a grouting slot and ventilation hole for filling the annular space between the sheath and the hole with cement. Finally, it can grouted cement or other sealants from the secondary grouting hole to fill the void beneath the anchor head (Fig. 2d). Because the materials used in the smart anchor are the same as those used in conventional assembly methods (e.g., steel strands, cement, and plastic sheaths), they can be easily accepted by designers and contractors. In addition, if the blockage of the leakage sources and the operation procedures can be effectively implemented, the requirements for permanent corrosion protection for ground anchors proposed by the British Standards Institution [14] can be satisfied (guarantee of fully corrosion-protected ground anchors).

Principle of self-inspection of anchor load change

The self-inspection function of the smart anchor was created based on the assembly method in Fig. 2. In the life cycle of a ground anchor, each strand in the free-length section can be extended. However, the reference strand, without lock-in wedges, is not connected to the anchorage head. When all the strands are of the same length and the exposed length is known, a relative displacement between the stressed strands and the reference strand (unstressed strand) indicates a change in the anchor load. Although the principle of the loading inspection of smart anchor is similar to that of a tell-tale device, the reference strand is not as difficult to install as a tell-tale device is during construction because it is a part of the assembly like the other strands. Fig. 3a displays the initial state of self-inspection of load change of the smart anchor. Considering the size of the anchor head commonly used in Taiwan, we set the designed exposed length to be 15–20 cm. The reference strand could reflect the state of load increase or decrease. When the slope moves outwards, the load on the anchor increases, and the reference strand becomes relatively shorter than the engaged strands (Fig. 3b). By contrast, when the load on anchor decreases because of slope material creep, anchor material creep, or anchor corrosion, the reference strand becomes relatively longer than the engaged strands (Fig. 3c). This concept was proven feasible by Liao et al. through an on-site stress test [11]. Anchor load change (ΔP) can be estimated by Eq. (1). The accuracy of the estimation had an approximately 2 %–5% error compared with that produced by a lift-off test.

$$\Delta P = \frac{\delta \times E \times \sum A}{L_{eff}} \tag{1}$$

where δ is the relative displacement of the reference strand in response to the anchor load change (cm); E is the Young's modulus of steel strands (2000 t/cm^2); $\sum A$ is the sum of cross-sectional area of all engaged steel strands (the diameter and cross-sectional area of the steel strands commonly used in ground anchors are 12.7 mm and 0.9871 cm^2, respectively); and L_{eff} is the designed free-length of a ground anchor. Furthermore, when anchor load change (ΔP), whether an increase or a decrease, the residual load (P_r) of a ground anchor can be estimated by

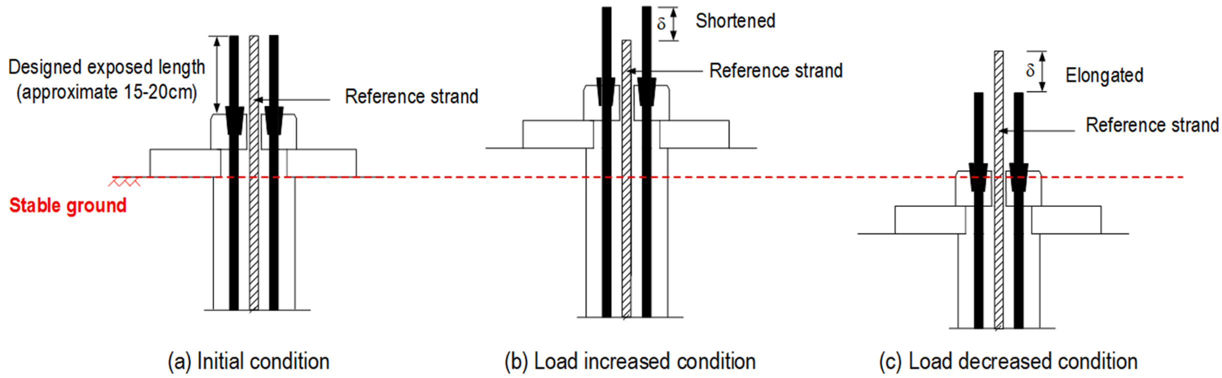

Fig. 3. Self-inspection for anchor load change of the smart anchor: (a) initial condition; (b) load-increased condition; (c) load-decreased condition.

adding the initial locked-in load of the ground anchor (P_i):

$$P_r = P_i + \Delta P \quad (2)$$

where P_i is the initial locked-in load of a new ground anchor (or residual load for existing anchor), which is typically designed to be 1.1–1.2 deigned load (T_w).

Different from commercial monitoring systems, the self-inspection function of the smart anchor enables manual value reading without additional components. Moreover, when detected a loss in anchor load, restressing can be applied to the non-engaged reference strand to supplement the anchor load if other components are complete and not corroded. In other words, the smart anchor is anti-corrosive, has a self-inspection function for load change, and facilitates maintenance for restressing.

Automating the self-inspection function of the smart anchor

To transform the mechanical loading inspection function into a device with an automation function as with other commercial systems, an additional linear potentiometer, data logger, power supply, and data transmitter can be mounted on the anchor head, a visible position that is convenient for maintenance. The composition and the suitable range for anchor load monitoring are elaborated as follows:

Components of automated self-inspection device

Originally, the load change estimation of the smart anchor was performed manually. Engineers must visit the site, remove the protective cap from the anchor head, and measure the relative displacement between the engaged strands and the reference strand. Transforming the load change estimation of the smart anchor into automated monitoring

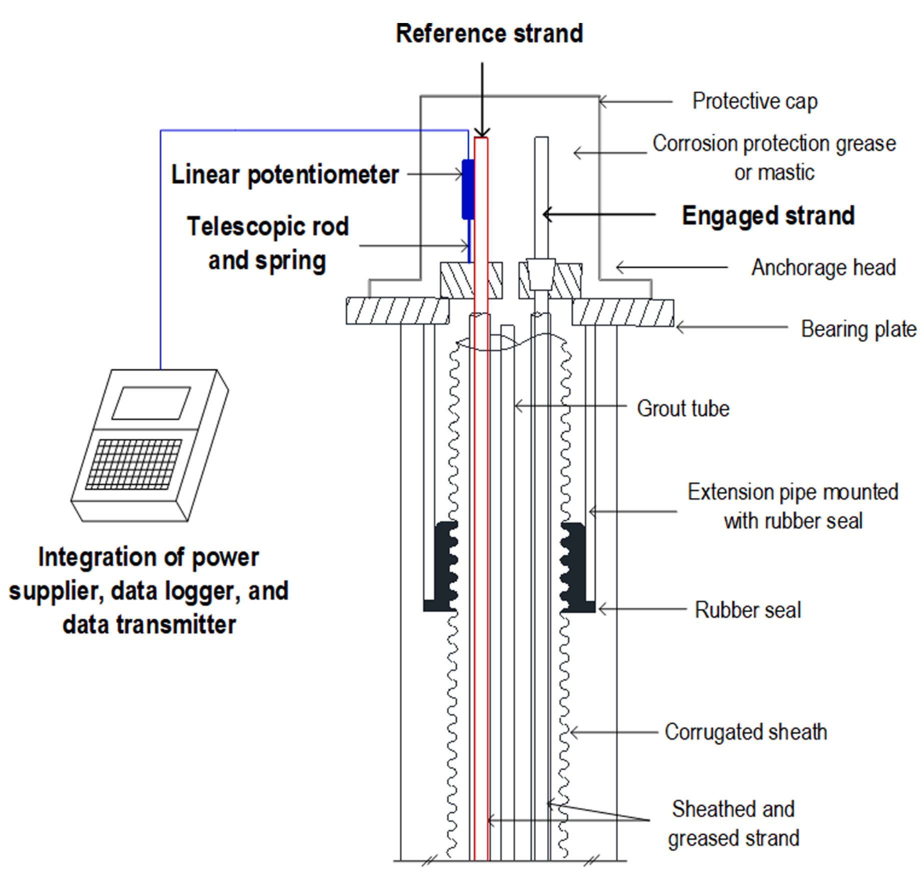

Fig. 4. Main components of the automated self-inspection device on the anchorage head.

would reduce maintenance costs; allow engineers to observe, almost in real-time, load changes of the complete anchored system. In addition to the reference strand on the smart anchor, a linear potentiometer, power supply, data logger, and data transmitter are mounted on the anchor head in the same manner as the commercial system (Fig. 4). Following are characterizes of the automated device:

(1) Linear potentiometer: A device installed on the reference strand to automatically measure the relative displacement between the engaged strands and the reference strand. The size of a linear potentiometer and the effective travel length is flexible, but they should be within the space limitations in the protective cap of the anchor head (typically within 25 cm) and should be waterproof, grease-resistant, and easy to assemble and disassemble. Fig. 5a is a photo of a linear potentiometer mounted on a reference strand. The extension rod is equipped with a spring to control the value reading of the linear potentiometer when the anchor load increases or decreases.
(2) Integration of the power supply, data logger, and data transmitter: Low energy consumption, high transmission, and high expandability (compatibility of different sensing devices) are the current trends in the development of monitoring systems. The commercial integrated device was used in this study can receive data from four sensor nodes simultaneously and be set to save data in the logger or transmit it wirelessly through the sensor nodes; the data can also be downloaded manually using a mobile application. As illustrated in Fig. 5b, the device is powered by 3.6-V lithium batteries. Under normal conditions, if the four nodes operate simultaneously and the sampling rate is set to 30 min, the power supply can last for more than two years.

Suitable range for anchor load change monitoring

The key factors affecting the automatic monitoring of the smart anchor are the effective travel length and sensitivity of the linear potentiometer. Although the effective travel length is flexible as long as it complies with the height of the protective cap, it recommends taking the designed load (or the residual load) of ground anchor into account; because of both an excessively long and short effective travel length are not adequate. For example, according to the score criteria of residual anchor load by the Taiwan Freeway Bureau [15], if the designed load of a ground anchor is 45 t, the Young's modulus of its strand ($E = 2000$ t/cm^2), the cross-sectional area ($A = 6 \times 0.9871$ cm^2), and the effective free-length (12 m) are all known conditions. Therefore, the elongated length and shortened length of the reference strand under different residual loads can be estimated by using Eq. (1) and Eq. (2), and the effective travel length of the linear potentiometer can be determined according to the result. As summarized in Table 1, when the residual anchor load reaches a critical level (Level A), the anchor load may increase to more than 1.2 T_w (54 t) or decrease to less than 0.2 T_w (9 t). The linear potentiometer must then be able to shorten by 0.87 cm (compressible length) or increase by 3.47 cm (extensible length), respectively. That is, the effective travel length of the linear potentiometer must exceed 4.31 cm. However, when the designed load of the ground anchor, the effective free-length, or the cross-sectional area of the strands is adjusted, the effective travel length of the linear potentiometer (the sum of the compressible length and the extensible length) must be suitably modified according to the needs of the site.

Application to field anchors in freeway-side anchored slopes

To verify the applicability of the automatic monitoring for the smart anchor, this study performed a field test at freeway-side anchored slope. Furthermore, to confirm the reliability of the recorded data, we attached an electric load cell to the sensing anchor to synchronize recorded loading for verification. The site condition, characteristics of field anchors, device assembly, and recorded data were explained as follows:

Site condition and field anchors characteristics

The test site was located on an anchored slope above a tunnel entrance on Freeway 6 in central Taiwan (Fig. 6). The anchored slope is divided into left and right zones and is reinforced by a tie-back anchor system (installed 84 ground anchors). The geology condition of the test site consisted of gravel and sandstone–shale couplets with a favorable texture. Groundwater is not abundant, and the slope surface is equipped

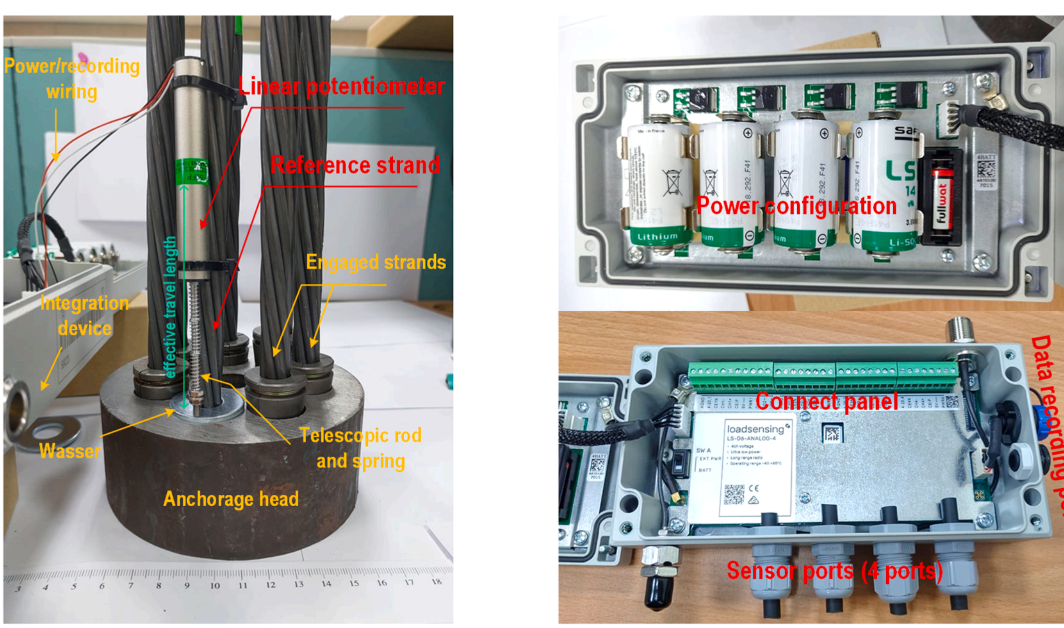

(a) Linear potentiometer mounted on reference strand

(b) Integration device (integrated with power supplier, data logger, data transmitter)

Fig. 5. Photo of: (a) linear potentiometer mounted on the reference strand and (b) integration device connected to the anchorage head.

Table 1
Effective travel length (shortened length and elongated length) corresponding to different grades of residual anchor load.

<table>
<tr><td>Grade of residual anchor load</td><td>According to Taiwan Freeway asset management handbook [15] definite, the grade of residual anchor load can be express as :
<table>
<tr><td>Grade</td><td>Fail (X)</td><td>Very poor (A)</td><td>Poor (B)</td><td>Fair (C)</td><td>Good (D)</td><td>Very poor (A)</td></tr>
<tr><td>Residual load (P_r)</td><td>0 T_w</td><td><0.2 T_w</td><td><0.5 T_w</td><td><0.8 T_w</td><td>=T_w</td><td>>1.2 T_w</td></tr>
</table></td></tr>
<tr><td>Condition of example ground anchor</td><td>If an example ground anchor have the design load=45 tons, the effective free-strand length= 1200 cm, the cross-sectional area of all engaged steel strands $\sum A = 5.9226$ cm^2 (A = 0.9871 cm^2 for a seven-wire strand with a nominal diameter of 12.7 mm), Young's modulus of steel strand = 2X10^6 kg/cm^2.</td></tr>
<tr><td>Corresponding shortened or elongated length to different grades of residual anchor load</td><td>
<table>
<tr><td>Grade</td><td>Fail (X)</td><td>Very poor (A)</td><td>Poor (B)</td><td>Fair (C)</td><td>Good (D)</td><td>Very poor (A)</td></tr>
<tr><td>Residual load (P_r)</td><td>0 ton</td><td>< 9 tons</td><td>< 22.5 tons</td><td>< 36 tons</td><td>45 tons</td><td>> 54 tons</td></tr>
<tr><td>Shortened (-) or elongated (+) length</td><td>-</td><td>> + 3.47 mm</td><td>> + 2.17 mm</td><td>> + 0.87 mm</td><td>0</td><td>< - 0.87 mm</td></tr>
</table></td></tr>
</table>

Fig. 6. Perspective view and sensing anchors in an anchored slope (freeway-side 6 in central Taiwan).

with a proper drainage system; therefore, no obvious corrosion was discovered in the ground anchors according to previous inspection results, and the load was kept at a stable level [16].

As shown in Fig. 6, two ground anchors were selected for sensing tests, one from the left (under direct sunlight side) and one from the right zones (not under direct sunlight side). The two sensing anchors were installed in 2015. They had a designed load of 45 t and a designed length of 40 m, where the free length section was 30 m and the fixed length section was 10 m. The construction materials and assembly method of those two sensing anchors were the same as those presented in Fig. 2. One of the strands served as reference strand, which was without locked-in wedge and used as a measuring component to assess anchor load changes (Fig. 7). Although the design of the sensing anchor has been well-established, the estimated value obtained by the self-inspection device of the sensing anchor requires a residual load for comparison according to Eq. (2). Therefore, before installing the automated device to activate the reference strand, we conducted a lift-off test to determine the value of residual load of the two sensing anchors to provide a reliable load reference value. The results of the lift-off test (Fig. 8) indicated that the residual loads of sensing anchor 1 and sensing anchor 2 were 54 t and 47 t, respectively.

Set up the automated recording devices on reference strand and anchor head

As mentioned above, the linear potentiometer is a key device for automated smart anchors. After determining the residual load of sensing anchors 1 and 2, a linear potentiometer with an effective travel length of 5 cm was attached to the reference strand of the two field anchors (compressible length: −1 cm; extensible length: 4 cm). When the load of the sensing anchor changes, the twisted strand will be displaced and accompanied by a certain degree of torsion of the anchorage head.

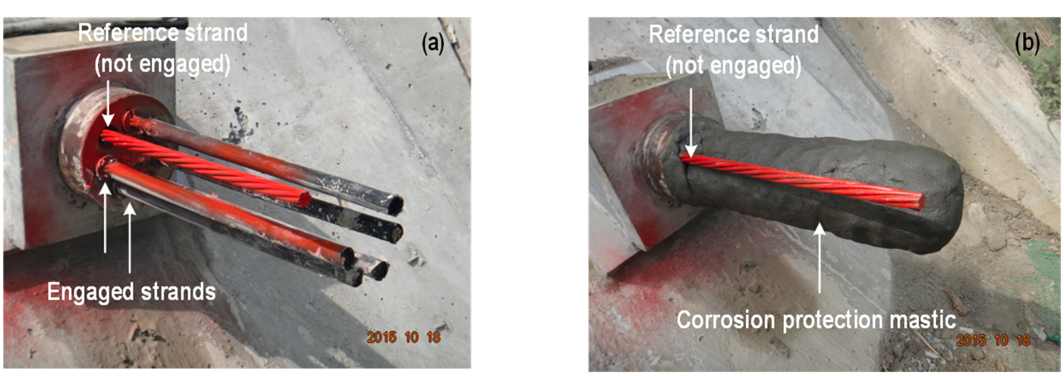

Fig. 7. The photo of a sensing anchor during installed: (a) reference strand and engaged strands and (b) engaged strands and anchor head protected with mastic.

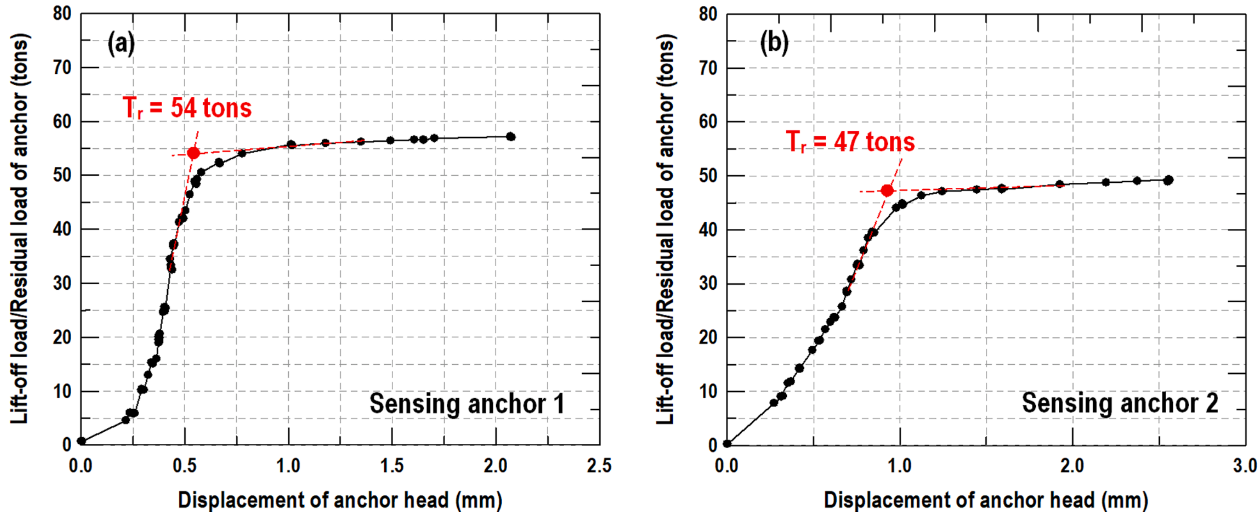

Fig. 8. Lift-off test result and residual load of: (a) sensing anchor 1 and (b) sensing anchor 2.

Therefore, to prevent the probe of the linear potentiometer from sliding into the wedge hole on the anchorage head and being twisted off, it had to cover the wedge hole with an appropriate washer (Fig. 9a). To verify the recorded obtained from the linear potentiometer and the reliability of the load estimated by Eq. (1) and Eq. (2), this study installed an electric load cell on the sensing anchors through a special steel seat to transmit the stress forces from the anchorage head to bearing plate 3 (Fig. 9b and Fig. 9d) and applied the integrated device to record data concurrently. After anticorrosion paste or grease was applied to the anchor head, we covered it with a protective cap. The power wring and the recording wring could pass through the designated hole on the protective cap and be connected to the integrated device (in the protective cover) with the power supply, data logger, and data transmitter (Fig. 9c).

Recorded data and environmental impact

The field test for the automated smart anchor began on July 30, 2019, and ended on June 9, 2020. It encompassed nearly-one year of seasonal temperature changes, with a high temperature of approximately 36 °C in summer and a low temperature of approximately 4 °C in winter. Recorded data in Fig. 10 indicates that for both sensing anchors 1 and 2, the load estimated by the linear potentiometer of the smart anchor and the data directly recorded by the electric load cell were consistent, which verified that the automated self-inspection of the smart anchor was reliable. However, after carefully inspecting the changes in the recorded data, it can be discovered that the value reading of the electric load cell was not as stable as that of the self-inspection device. The electric load cell was affected by the environmental temperature (Fig. 11). In general, the reading was lower when the ambient temperature decreased and higher when the ambient temperature increased. Also, we should pay attention that whether exposure to direct sunlight is an important factor to load cell reading, which is the sensing anchor 1 under direct sunlight. Relatively, sensing anchor 2 is not. As shown in Fig. 11, it can be seen that the load cell reading shift of sensing anchor 1 is about 2 times larger than that of sensing anchor 2. Based on this observation, when there is direct sunlight and constant temperature changes, the load cell reading on sensing anchor 1 has more significant

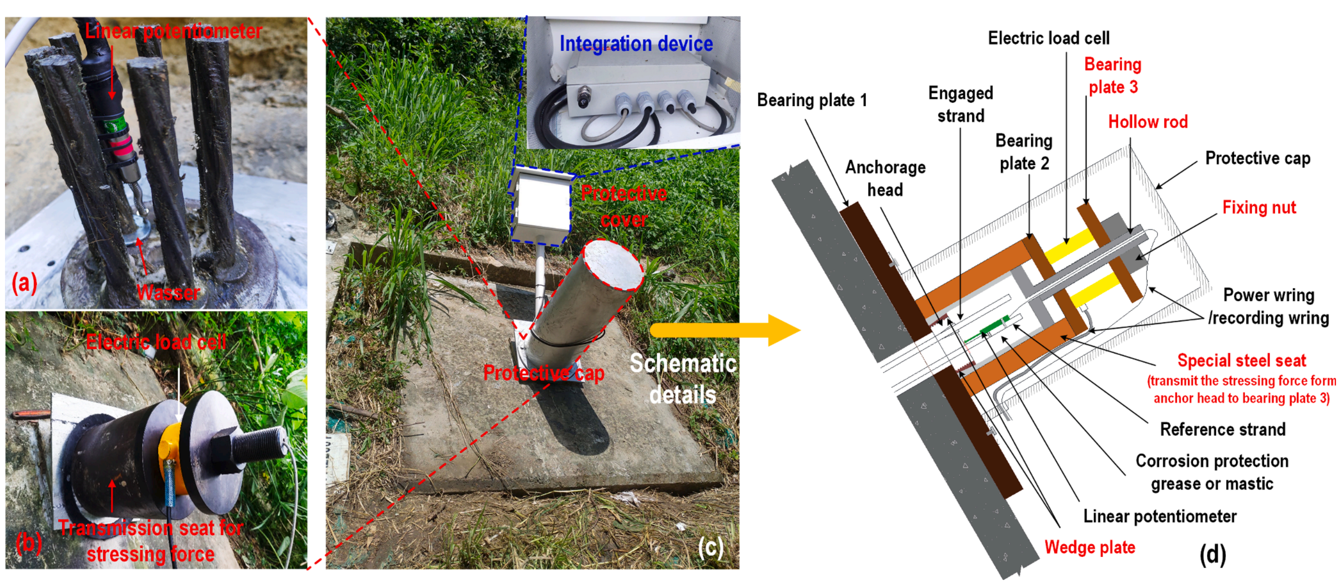

Fig. 9. Automated recording devices set up on the sensing anchors: (a) linear potentiometer mounted on the reference strand and washer placed on the wedge hole; (b) set up the special steel seat and electric load cell; (c) integrate device protected by the protective cover; (d) schematic of the automated devices in the protective cap.

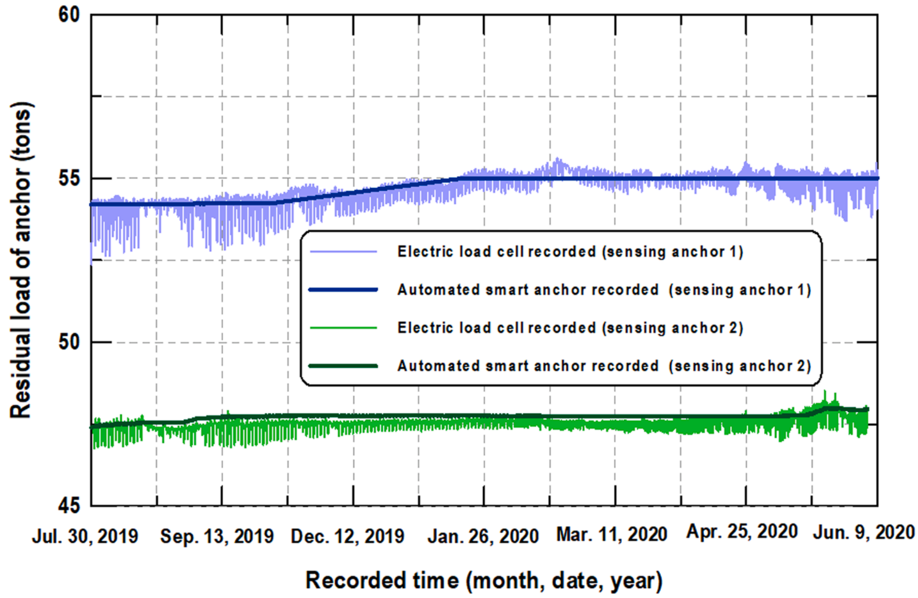

Fig. 10. Comparison of recorded data for the automated smart anchor and electric load cell from field sensing anchors 1 and 2.

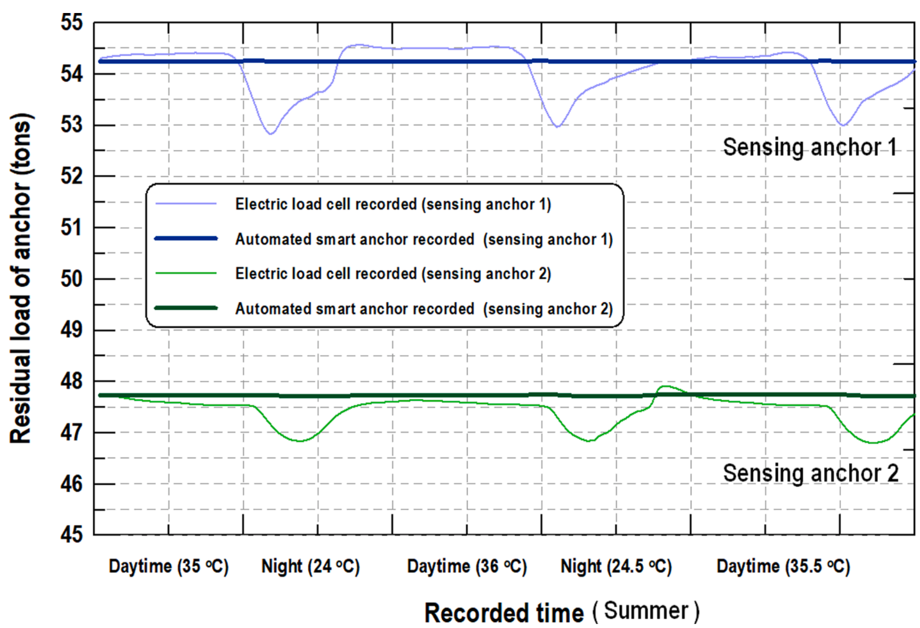

Fig. 11. Effect of environmental temperature on the recorded data for the automated smart anchor and the electric load cell.

shift than that on sensing anchor 2 (Fig. 10). This demonstrated that the zero point of the electric load cell shifts by ambient temperature changes after it is in service for some time; it must be removed for calibration to maintain a normal monitoring function. However, regular calibration is unworkable in practice; therefore, most long-term values provided by electric load cells are likely unstable.

Power supplies, data loggers, and data transmitters are fundamentally non-waterproof electronics, although they can be protected by protective covers (Fig. 9c). When the sensing anchors are located outside of the city, the problem of insects entering the protective covers should also be paid attention to. Insect secretions, excrement, or eggs may cause battery leakage, short circuits, or otherwise affect the service life of the devices. It recommends that strict protective measures (e.g., pest control and circuit board coating and packaging) be taken to ensure normal monitoring function (Fig. 12).

Discussion of field studies and future development

Compared to the electric load cell, the field test results verified that the automated self-inspection of the smart anchor was reliable and had a stable function. Based on experience from the field test, it can highlight the features of the automated self-inspection function of the smart anchor (1) the reference strand is a part of the anchor assembly like the other stands, it can be easily implemented during the assembly process with no limitations in installing equipment; (2) the reference strand serves as the self-inspection device, except the cost of wire material, no more extra cost of construction and sensor occur; (3) the self-inspection device on the smart anchor had a mechanical element that was not affected by ambient temperature and did not require calibration; (4) the whole system had to be waterproof, grease-resistant, and insect-resistant. As mentioned above, the smart anchor is worthy of practical applications.

Fig. 12. Environmental impacts on the integrated device and damage prevention in the field.

Some studies have applied geotechnical instruments, water level gauges, laser scanning, global positioning systems, and geographic information systems to implement slope safety monitoring and early warning systems [17–20]. They integrated multiple monitoring indicators, such as groundwater level, deformation, and geological evolution. In the smart anchor, although it did not use integrated indicators, the self-inspection system we proposed could monitor the load level and its changes, which is a critical factor for anchored slopes. The automated smart anchor is extensible. Vibrating wire and resistance sensing devices can be connected to the integration device. Moreover, as in commercially monitoring systems, an inspection IoT can be established using wireless to connect with sensor nodes and gateways. All types of monitoring data can be uploaded to an inspection platform to create an intelligent system with a pre-warning function (Fig. 13).

In Taiwan, inaccurate electric load cells are generally not disassembled for renewal or calibration. One of the reasons is cost-effectiveness considerations, the other is disassembly procedure of the electric load cell may change the engaged position of the lock-in wedges on steel strands (the bite marks and weak location shown as Fig. 14) and hinder corrosion prevention in tendon assembly. Therefore, most long-

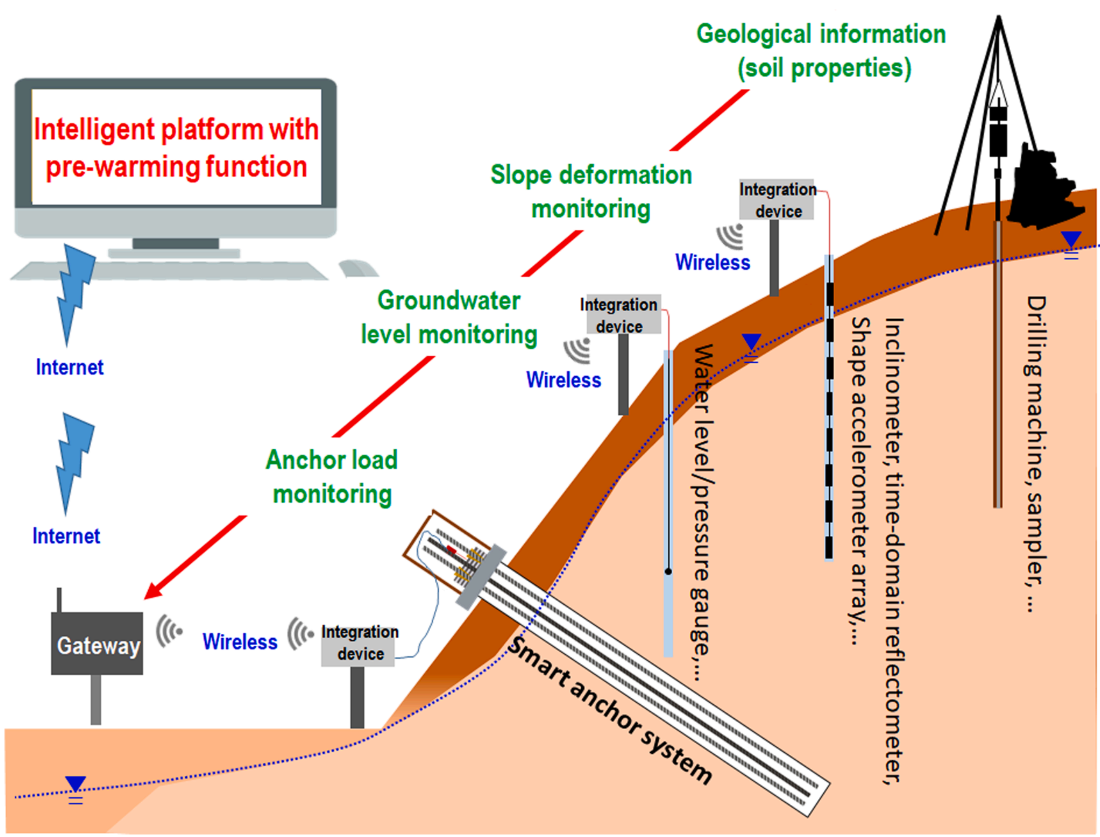

Fig. 13. Concept and future development of an intelligence platform for the smart anchor system.

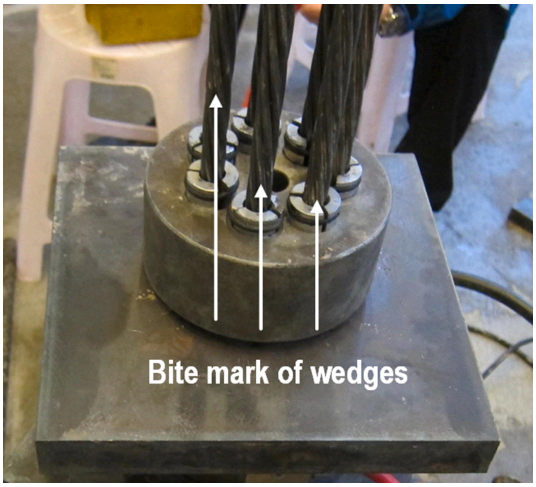

Fig. 14. Photo of a weak location and bite marks on the strand.

term values recorded from electric load cells are likely unstable, which makes the development of the automation smart anchor promising. At present, we detected the loss of anchors load is typically installing more anchors to increase the safety of the anchored slopes. However, the reference strand in smart anchor is not only used as a component for load measurements. When an anchor requires restressing, the reference strand also can be engaged with a lock-in wedge after stressing is applied without having to install more anchors [the maximum supplement stressing of each reference strand is approximately 18.7 (yield strength of steel strand at 0.1 % elongation) × 0.5 (minimum safety factor for tendon strands) = 9.35 t].

Conclusions

The automated self-inspection function on the smart anchor differs from commercial monitoring systems. It can perform the load monitoring of anchored slopes without having to install additional sensors. The near 1-year field monitoring results indicated that the automated smart anchor had high reliability and stability. Additionally, the reference strand on the smart anchor is in line with the sustainable development goals of anchor life cycle. It can perform re-stressing and positive benefit of maintenance. The following conclusions can be drawn from this study:

1) Corrosion is one of the common problems of ground anchors in Taiwan. The smart anchor assembly can satisfy the requirements of permanent anchors by being integrated. Furthermore, new materials, techniques, or equipment are not required for construction, so it can be easily accepted by designers and contractors.
2) The reference strand on the smart anchor can serve as the self-inspection device for long-term load change. Meanwhile, the reliability of automatic self-inspection capabilities for anchor load monitoring was demonstrated through two field sensing anchors. It would reduce maintenance costs and the engineers can contribute their expertise to value tasks.
3) Smart anchors have been solved by innovative assembly procedures. It features no limitations in installing equipment, and no extra cost of construction and sensor occurs. They are not affected by ambient temperature and did not require calibration. Although the whole system had to be waterproof, grease-resistant, and insect-resistant when being implemented on-site, the smart anchor is still worthy of practical applications.
4) In the field, insect invasion and survival responses (e.g., secretions, excrement, or eggs) are the main cause of short circuits and damage to electronic loggers. Appropriate protective measures are required (e.g., pest control for the protective unit and coating and packaging for circuit boards).
5) When a smart anchor detection requires restressing (detected a loss in anchor load), the reference strand can be engaged with a lock-in wedge after stressing is applied (maximum supplement load = 9.35 t/per strand). If necessary, it can rely on supplementary restressing instead of installing more anchors to increase the safety of the anchored slopes. It has the positive benefit of maintenance in the anchor life cycle.

CRediT authorship contribution statement

Shih-Hao Cheng: Conceptualization, Methodology, Writing – original draft, Writing – review & editing, Data curation, Validation. **Shi-Shuenn Chen:** Supervision, Writing – review & editing. **Kuo-Hsin Yang:** Writing – review & editing.

Declaration of Competing Interest

The authors declare that they have no known competing financial interests or personal relationships that could have appeared to influence the work reported in this paper.

Data availability

The data that has been used is confidential.

Acknowledgments

The authors thank the Taiwan Freeway Bureau (Central Region Engineering Office) for providing financial support and test sites to perform the experiments on smart anchors (No. 108C010C016). The authors also thank Distinguished Professor Hung-Jiun Liao for sharing his valuable ground anchor construction and research experience, and the local ground anchor contractors and engineers who performed the inspection and remediation work on numerous anchored slopes. Finally, the authors are also thankful for the support of the Taiwan Building Technology Center from the Featured Areas Research Center Program funded by the Ministry of Education in Taiwan.

References

[1] Liao HJ. Forensic Study on the Dip Slope Failure at Chainage 3.1k of National Freeway No.3. Chinese Taipei Geotechnical Society 2011. in Chinese.
[2] Liao HJ, Cheng SH. Failure types and treatment of anchored slopes in northern Taiwan. Sino-Geotechnics 2011;130:7–18. in Chinese.
[3] Liao HJ, Lee WF, Wang CW. A tale of twin cut slopes in Taiwan. Proc Inst Civil Eng Forens Eng 2013;166(2):72–80.
[4] Liao HJ, Cheng SH. Overhaul the anchored slopes in Taiwan. In: Hazarika H, Kazama M, Lee WF, editors. Geotechnical Hazards from Large Earthquakes and Heavy Rainfalls. Tokyo: Springer Japan; 2017. p. 269–80.
[5] Catane SG, Mark AH, Zarco CJ, Cordero N, Roy AN, Kaimo RM, et al. Laboratory experiments on steady state seepage-induced landslides using slope models and sensors. Sci Diliman 2011;23:17–30.
[6] P. Fabo, M. Chandoga, A. Jarosevic: The smart tendons a new approach to prestressing. In: Fib Symposium, Avignon, France (2004).
[7] Islam S, Purinton K. Long-term force monitoring of prestressed anchors used on dam rehabilitation projects. In: Dam Safety 2015 Conference, New Orleans, LA, USA; 2015.
[8] Liao HJ. Guidelines for the Geotechnical Facilities Maintenance and Management of Highway Slopes. Chinese Taipei Geotechnical Society 2014. in Chinese.
[9] Liao HJ, Cheng SH, Chen CC, Chen HR. Cement grouting to seal off voids below anchor head. In: Grouting, Deep Mixing and Diaphragm Walls at Grouting 2017, Hawaii USA, July, GSP 287 303–313. https://doi.org/10.1061/9780784480786.030.
[10] Dunnicliff J. Geotechnical Instrumentation for Monitoring Field Performance. Chichester, U.K.: Wiley; 1988.
[11] Liao HJ, Cheng SH, Chen HR, Chen CC. Simple method to measure the long-term load change of ground anchors. Geotech Test J 2017;40:345–50.
[12] Liao HJ, Cheng SH, Chen CC, Chen RD. Remedial measures for existing anchored slopes in Taiwan. J Perform Constr Facil 2019;33:04019027-1–04019027-11. https://doi.org/10.1061/(ASCE)CF.1943-5509.0001295.

[13] Xu DS, Yin JH. Analysis of excavation-induced stress distributions of GFRP anchors in a soil slope using distributed fiber optic sensors. Eng Geol 2016;213:55–63. https://doi.org/10.1016/j.enggeo.2016.08.011.

[14] British Standard Institute (BSI), Code of Practice for Ground Anchorages BS 8081 London, U.K., 2015.

[15] Taiwan Freeway Bureau, Asset management handbook, Taipei, Taiwan, 2018.

[16] Taiwan Freeway Bureau (central office), Technical report of slope inspection/monitoring and ground anchor inspection work in freeway No. 3 and No. 6, Taichung, Taiwan, 2018.

[17] Dai FC, Lee CF. Landslide characteristics and slope instability modeling using GIS, Lantau Island, Hong Kong. Geomorphology 2002;42:213–28. https://doi.org/10.1016/S0169-555X(01)00087-3.

[18] Ayalew L, Yamagishi H, Marui H, Kanno T. Landslides in Sado Island of Japan: Part I Case studies, monitoring techniques and environmental considerations. Eng Geol 2005;81:419–31. https://doi.org/10.1016/j.enggeo.2005.08.005.

[19] Oh HJ, Lee S. Landslide susceptibility mapping on Panaon Island, Philippines using a geographic information system. Environ Earth Sci 2011;62:935–51. https://doi.org/10.1007/s12665-010-0579-2.

[20] Pradhan B, Chaudhari A, Adinarayana J, Buchroithner MF. Soil erosion assessment and its correlation with landslide events using remote sensing data and GIS: a case study at Penang Island, Malaysia, Environmental monitoring and assessment 184. Environ Monit Assess 2012;184(2):715–27.